

Local spin polarization in ballistic quantum point contacts

Chuan-Kui Wang and K.-F. Berggren

Department of Physics and Measurement Technology, Linköping University, S-58183 Linköping, Sweden

(Received 13 May 1997)

Self-consistent calculations of the electronic structure and conductance of a ballistic quantum point contact (QPC) in the one-subband limit are reported. The spin-polarized density-functional theory of Kohn-Sham is used. The self-consistent results show that spontaneous spin polarization occurs locally in the region of the saddle point as the electron density is lowered. As a consequence, the effective potential barriers become different for spin up and spin down electrons. Transport associated with spin up electrons, let us say, then suddenly takes place via tunneling, while spin down electrons still carry the current via propagating states in a normal way. The onset of spontaneous spin polarization induces anomalies in the conductance. Our results support the recent interpretations of experimentally observed conductance anomalies in QPCs near pinch off. The agreement with measurements is qualitative, however, rather than quantitative. Reasons for the discrepancy are proposed. [S0163-1829(98)02608-3]

The number of electrons in a quantum point contact (QPC), i.e., a short constriction connecting two electron reservoirs, may be quite small close to pinch off. This suggests that electron interactions become especially important as the conductance is lowered below $G = 2e^2/h$, the lowest conduction plateau. Recent conductance measurements by Thomas *et al.*¹ for low-dimensional split gate QPCs in modulation-doped high-mobility GaAs/Al_xGa_{1-x}As heterostructures have revealed a conductance anomaly at $G \approx 0.7(2e^2/h)$. This feature, which has been recorded also in some previous measurements^{2,3} but has passed unmentioned so far, was interpreted by Thomas *et al.* in terms of spontaneous spin polarization. Additional support for the idea that electron interactions play an increasingly important role when only a few subbands are occupied comes from the observed enhancement of the effective electron g factor above the bulk value for GaAs.¹ The alternative explanation that the structure would be caused by, e.g., the presence of impurities in the vicinity of the QPC, as studied in detail by McEuen *et al.*,⁴ is excluded for the following reasons. The anomaly has been seen in a large number of high-mobility samples and the effect is reproducible on cooldowns. In the case of an impurity, the measured structure in G was found to disappear on thermal cycling.⁴ Then there is the magnetic field effect showing evolution of “0.7 structure” to 0.5 on increasing parallel magnetic field. The results were also checked for possible impurity effects by shifting the position of the channel sidewise.

Conductance anomalies supporting the idea of spontaneous spin polarization have also been observed by Tscheuschner and Wieck⁵ for GaAs/Al_xGa_{1-x}As heterostructure in-plane-gate (IPG) transistors using focused-ion-beam implantation techniques. In this case, the anomaly is found at $G \approx 0.5(e^2/h)$ for zero bias and zero external magnetic field. Deviations from exact quantization of the first normal plateau are, however, noted. Most recently the conductance anomaly has been observed also for a short regrown Ga_{0.25}In_{0.75}As/InP quantum wire by Ramvall *et al.*⁶ In addition, a conductance plateau is also observed at $\sim 0.2(2e^2/h)$. Both the structures at $0.7(2e^2/h)$ and

$0.2(2e^2/h)$ evolve into a plateau at $0.5(2e^2/h)$ if the sample is subject to an in-plane magnetic field. [In fact, Ramvall *et al.* also report on a higher plateau at $1.5(2e^2/h)$. Since we will be concerned with single mode events only, we will not comment on it further.] Anomalous structures for conductances below $(2e^2/h)$ and their dependence on source-drain voltage have been discussed previously by Patel *et al.*⁷

In the limit of single-mode conduction, a QPC may be considered as a quasi-one-dimensional (1D) system, at least locally. One candidate for modeling the low-temperature properties of such a system is the Tomonaga-Luttinger liquid theory for locally interacting 1D electrons.⁸ The conductance in the presence of mutual interactions is then renormalized as $K(2e^2/h)$, where K is the interaction-dependent parameter characterizing the Tomonaga-Luttinger liquid. For repulsive or attractive interactions, $K < 1$ and $K > 1$, respectively; $K = 1$ refers to noninteracting electrons. Other theories⁹⁻¹¹ based on the Tomonaga-Luttinger model claim that the conductance renormalization will not occur, which would explain Tarucha's experimental results¹² for long quantum wires. As it appears, the Tomonaga-Luttinger model is not immediately successful in explaining the observed conductance anomaly.¹ To connect to real experimental systems one has to take into account finite-size and boundary effects. In addition, real systems are quasi-one-dimensional in contrast to the strictly 1D Tomonaga-Luttinger model. Here we will therefore follow another way of analyzing transport in the one-mode limit of a QPC. Hence we will use methods based on the Kohn-Sham equations. Methods of this kind are well established for modeling realistic quantum structures in the nanometer regime.

In our previous study¹³ of infinite ballistic quantum channels, spontaneous spin polarization driven by the exchange interaction between the electrons was generally found to occur at low subband fillings. In such situations exchange dominates over kinetic energy. As a consequence, the ground state turns into a fully spin-polarized state in analogy with the well studied three-dimensional electron gas.¹⁴ Similar results have been obtained for single mode cylindrical quantum wires.¹⁵⁻¹⁷ Apparently these findings seem to support

the interpretation of Thomas *et al.*¹ of the observed conductance, anomaly. On the other hand, it is a gross oversimplification to model a real QPC with an idealized infinite channel. The purpose of the present work is therefore to demonstrate that spin polarization may indeed occur also in a QPC with a more realistic geometry. Below we will present a self-consistent calculation of the electronic structure of a ballistic QPC in the limit of a single open mode and show how spontaneous spin polarization can occur locally in the region of the QPC itself. Once the spin polarization takes place, the potential barrier for one of the spin directions is suddenly increased and may exceed the Fermi level. The transport associated with this spin then takes place via tunneling through an exchange-enhanced barrier. For electrons with opposite spin the barrier remains relatively unchanged and the corresponding transport takes place in propagating states above the subband threshold in a normal way. The polarization occurs fairly abruptly over a narrow energy region and therefore induces an anomalous structure in the conductance. However, in view of the various approximations introduced in this first study of spontaneous spin polarization in a QPC, our analysis is meant to be qualitative rather than quantitative.

In the following we assume the following basic model for a QPC created by laterally confining a two-dimensional (2D) electron gas residing at a semiconductor interface, say, GaAs/Al_xGa_{1-x}As. The electron gas is assumed to be strictly 2D, i.e., the motion perpendicular to the interface is neglected. To simplify the numerical work further, we let our system consist of an infinite channel in which there is a short constriction defining the the actual QPC. A structure of this kind may be achieved by lateral electrostatic confinement, for example. Regions to the left and right of the constriction may be regarded as reservoirs serving as source and drain. The bare potential associated with the electrostatic confinement is qualitatively of the form

$$V_{\text{conf}}(x,y) = \frac{1}{2}m^*\omega_y^2 y^2 + \frac{V_0}{\cosh^2(\alpha x)}. \quad (1)$$

Here the first term to the right defines a straight channel extending in the x direction. The strength of the transverse confinement is defined by $\hbar\omega_y$. Subband thresholds or sublevels due to the transverse motion are $E_n = \hbar\omega_y(n + 1/2)$, with $n = 0, 1, 2, \dots$. Typical values for $\hbar\omega_y$ are in the range $\sim 1-2$ meV. The second term in Eq. (1) describes a saddle of height V_0 . In practice, V_0 may be regulated by electrostatic potentials, for example by an applied gate voltage. Therefore, the value of the bare potential at the saddle, V_0 , may be thought of as directly representing the influence of an applied gate voltage, i.e., the value of V_0 may be assumed to increase when the gate voltage is lowered. When considering transport, the region around the maximum is the important one. Expanding for small x we thus have

$$V_{\text{conf}}(x,y) \simeq \frac{1}{2}m^*\omega_y^2 y^2 - \frac{1}{2}m^*\omega_x^2 x^2 + V_0 \quad (2)$$

with $\omega_x = \sqrt{2\alpha V_0/m^*}$. This is the usual Büttiker¹⁸ saddle-point potential for a QPC used extensively for characterization of real devices from transport measurements (see, e.g., Refs. 7 and 19). In practice, ω_x is found to be of the same

order as ω_y . The potentials in Eqs. (1) and (2) are attractive from a calculational point of view. The solutions to the one-electron Schrödinger equation are separable and available analytically, i.e., the wave function is of the form $\varphi_{n,k}(x,y) = \Psi_n(y)\Phi_k(x)$ for states belonging to the n th subband.

Depending on the electron concentration, one or more subbands may be occupied. When many subbands become occupied, electrostatic and exchange interactions will modify the effective potential. Because of the Hartree potential, the initially bare parabolic confinement potential will thus become a ‘‘split parabola,’’ i.e., an essentially flat region will develop at the bottom of the well (see, e.g., Ref. 13) while the walls of the well remain parabolic with the same curvature as the unperturbed parabola. To simulate a potential of this kind, one may use the Kohn-Sham equations.²⁰ The computational effort for the general case is, however, quite substantial. We will therefore simplify our problem by assuming that only the lowest subband is occupied. Our previous work¹³ shows that the Hartree term plays an insignificant role in this limit of low electron concentrations and we will therefore ignore this term. The effective Schrödinger therefore simplifies to

$$\left[\frac{p_x^2 + p_y^2}{2m^*} + V_{\text{conf}}(x,y) + V_{\text{exch}}^\sigma(x,y) \right] \varphi^\sigma(x,y) = E^\sigma \varphi^\sigma(x,y), \quad (3)$$

where $\sigma = \pm \frac{1}{2}$ refers to spin. In the Kohn-Sham local-density approximation (LDA), the exchange potential energy is²¹

$$V_{\text{exch}}^\sigma(x,y) = - \frac{e^2}{\epsilon_0 \epsilon \pi^{3/2}} (n^\sigma(x,y))^{1/2}, \quad (4)$$

where ϵ is the dielectric constant of the semiconductor material and $n^\sigma(x,y)$ is the spatial distribution for σ -spin electrons.

Because of the form of the exchange energy in Eq. (4), solutions to the effective Schrödinger equation are no longer separable. Considering, however, that the potential in the x direction is smooth, we may make use of the adiabatic approximation²² to write the wave function for the n th mode as

$$\varphi_{n,k}^\sigma(x,y) \simeq \Psi_n^\sigma(x,y)\Phi_k^\sigma(x). \quad (5)$$

Inserting this form into Eq. (3) and neglecting $\partial\Psi_n^\sigma/\partial x$ and $\partial^2\Psi_n^\sigma/\partial x^2$ because we expect them to be small, we may approximately decouple our problem as

$$\begin{aligned} & - \frac{\hbar^2}{2m^*} \frac{\partial^2}{\partial y^2} \Psi_n^\sigma(x,y) + [V_{\text{conf}}(x,y) + V_{\text{exch}}^\sigma(x,y)] \Psi_n^\sigma(x,y) \\ & = E_n^\sigma(x) \Psi_n^\sigma(x,y) \end{aligned} \quad (6)$$

for the transverse motion with ‘‘local’’ energy $E_n^\sigma(x)$ and

$$\frac{\partial^2}{\partial x^2} \Phi_k^\sigma(x) + (k^\sigma(x))^2 \Phi_k^\sigma(x) = 0 \quad (7)$$

for the translational motion with local energy $\epsilon_k^\sigma(x) = \hbar^2(k^\sigma(x))^2/2m^* = E^\sigma - E_n^\sigma(x)$. The transverse energy $E_n^\sigma(x)$ now acts as an effective, renormalized potential that

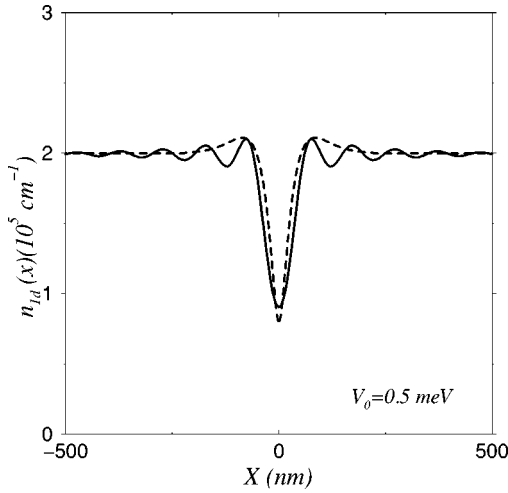


FIG. 1. Comparison of the exact, oscillatory electron density $n_{1D}(x)$ corresponding to the bare potential in Eq. (1) with the semiclassical type of approximation, Eq. (11), used in this work.

the translational states $\Phi^\sigma(x)$ with energy $\epsilon_k^\sigma(x)$ have to penetrate. Thus we obtain the transmission through the QPC for a single electron with energy E^σ by solving Eq. (7) once $E_n^\sigma(x)$ is known from Eq. (6). Because of the exchange potential, the problem has to be solved self-consistently for all the electrons occupying the lowest subband, i.e., the local electron distribution in the exchange potential in Eq. (4) is

$$n^\sigma(x, y) = \sum_k |\Phi_k^\sigma(x)|^2 |\Psi_1^\sigma(x, y)|^2. \quad (8)$$

Integrating over the normalized transverse function $\Psi_1^\sigma(x, y)$, the total 1D electron density is obtained,

$$n_{1D}(x) = \sum_\sigma n_{1D}^\sigma(x) = \sum_\sigma \sum_k |\Phi_k^\sigma(x)|^2 \quad (9)$$

with asymptotic limits

$$n_{1D}(\pm\infty) = \sum_\sigma \frac{1}{\pi} \left(\frac{2m^*}{\hbar} [E_F - E_1^\sigma(\pm\infty)] \right)^{1/2}. \quad (10)$$

Solving the Kohn-Sham equations numerically, we first slice the channel along the x direction, and then find the self-consistent solutions of Eq. (6) for each slice. For a given energy, E^σ , the solutions of Eq. (7) are used to calculate the electron distribution. With new electron distribution we need to solve Eqs. (6) and (7) once more in the same order and with the subsidiary constraint that the asymptotic value of $n_{1D}(\pm\infty)$ and the chemical potential of the reservoirs are being held fixed. Self-consistency is reached when the Fermi energies E_F in successive iterations are identical within a given numerical accuracy ($\sim 10^{-4}$ meV). As may be expected, $n_{1D}(x)$ displays 1D Friedel oscillations. The reason is that the constriction defining the QPC acts as a local potential perturbing the electron gas in the channel.

The self-consistent calculations are somewhat cumbersome because one has to include many states. As argued above, we only expect smooth variations and therefore introduce an approximate form for $n_{1D}(x)$ based on simple semiclassical arguments,

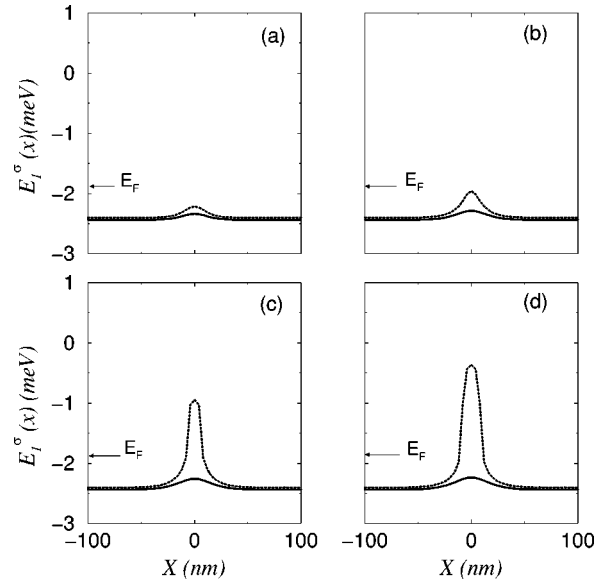


FIG. 2. Effective potential barriers along the x direction in a QPC for $n_{1D} = 2 \times 10^5 \text{ cm}^{-1}$. (a) $V_0 = 0.1$ meV; (b) $V_0 = 0.15$ meV; (c) $V_0 = 0.18$ meV; (d) $V_0 = 0.20$ meV, where V_0 is the potential at the saddle point. Dotted and solid lines correspond to spin up and spin down electrons, respectively. For technical reasons we have included the Zeeman splitting from a very weak external magnetic field in order to trigger the onset of spin polarization. Therefore, one finds a minor spin splitting also in the regions away from the QPC. Since this feature is due entirely to the Zeeman effect, it may be disregarded in present circumstances.

$$n_{1D}(x) = \sum_\sigma \left[\frac{k_F^\sigma}{\pi} + \frac{1}{4\pi(x_0 - x)} (1 - \exp^{-2q^\sigma(x_0 - x)}) + \frac{1}{4\pi(x_0 + x)} (1 - \exp^{-2q^\sigma(x_0 + x)}) \right], \quad (11)$$

where $k_F^\sigma(x) = \{2m^*/\hbar^2 [E_F - E_1^\sigma(x)]\}^{1/2}$, $q^\sigma(x) = [(2m^*/\hbar^2)E_1^\sigma(x)]^{1/2}$, and x_0 is an effective width of the barrier. Approximate and exact results for the bare barrier are shown in Fig. 1. Evidently the semiclassical method gives fair, averaged results for $n_{1D}(x)$ and may therefore be used to reduce the computational effort significantly. The price is, however, that the Friedel oscillations are lost. We will comment on this below.

Input parameters in the calculations are $m^* = 0.067m_e$ and $\epsilon = 13.1$, which are appropriate values for the GaAs/Al_xGa_{1-x}As interface. Furthermore, we choose $\hbar\omega_y = 2$ meV and $\hbar\omega_x = 1$ meV, which are typical values for nanostructures of the kind we consider here. Figure 2 shows the effective potential barriers for up and down spin electrons for different choices of barrier height V_0 when $n_{1D}(\pm\infty) = 2 \times 10^5 \text{ cm}^{-1}$. With this choice of electron density, only the lowest subband is occupied in the entire system, i.e., in the two ‘reservoirs’ as well as in the QPC itself. All cases in Fig. 2 show that spontaneous spin polarization occurs in the saddle region, but that a swift transformation to strong polarization takes place when the electron density is decreased by quite modest variations in the value for V_0 . Corresponding electron densities are displayed in Fig. 3. For $V_0 = 0.1$ and 0.15 meV, cases (a) and (b), respectively, the

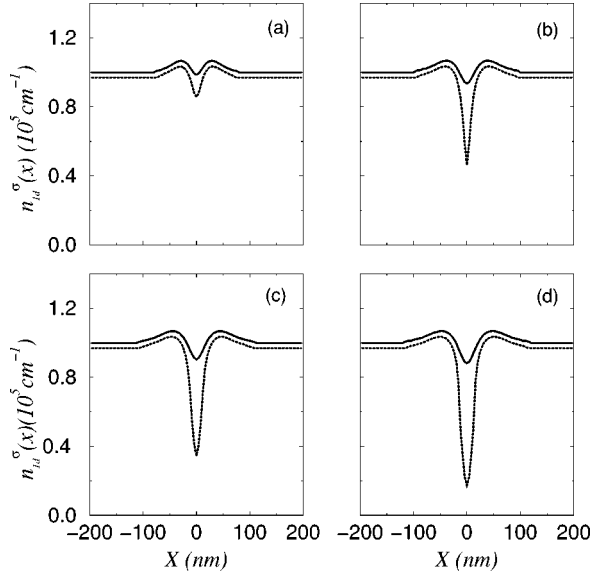


FIG. 3. One-dimensional electron densities $n_{1D}^{\sigma}(x)$ for the two spin directions. (a) $V_0=0.1$ meV; (b) $V_0=0.15$ meV; (c) $V_0=0.18$ meV; (d) $V_0=0.20$ meV. The asymptotic value of the electron density is $n_{1D}=2\times 10^5$ cm $^{-1}$. Dotted and solid lines correspond to spin up and spin down electrons, respectively. A weak Zeeman splitting is included as in Fig. 2.

Fermi level is higher than the barrier for both directions of spin. Therefore, electrons conduct current via propagating states in a normal way. As a consequence, the conductance is unaffected by the spin polarization and one finds the usual value $G=2e^2/h$. However, on further increase of V_0 , cases (c) and (d) in Fig. 2 for $V_0=0.18$ and 0.20 meV, respectively, show how the barriers for up and down spins rapidly become very different in the saddle region. The barrier for spin down electrons thus remains more or less unaffected by the exchange interactions while the barrier for spin up electrons becomes much larger than the Fermi energy. Figure 3 shows the corresponding 1D electron densities for increasing V_0 .

With the onset of strong local spin polarization, the conduction mechanism is, of course, altered in a profound way. Electric transport by spin up electrons must then take place via tunneling, while spin down electrons still contribute to the current by normal, propagating modes above the (local) subband threshold. By calculating transmission coefficients for the single-particle states and using the Landauer-Büttiker expression we have determined the conductance for the cases of noninteracting and interacting electrons as shown in Fig. 4. Clearly, the onset of spontaneous spin polarization manifests itself as an anomalous structure in the conductance which drops by $\sim 0.5(2e^2/h)$ over a narrow range. The details of the anomaly appear, however, to be dependent on geometry. For smaller values of $\hbar\omega_x$ than in our example in Fig. 4, i.e., for smaller ratio ω_x/ω_y , the QPC region is more extended in the x direction. The half plateau in G then becomes broader and more well defined. This is consistent with the results for an infinite channel.¹³ On the other hand, if we let $\hbar\omega_x$ take a larger value we may say that the effective length of the QPC is shorter. On increasing V_0 the onset of spin polarization then occurs in the range $0.5(2e^2/h)\leq G\leq(2e^2/h)$. Saturation is found in the range $0\leq G$

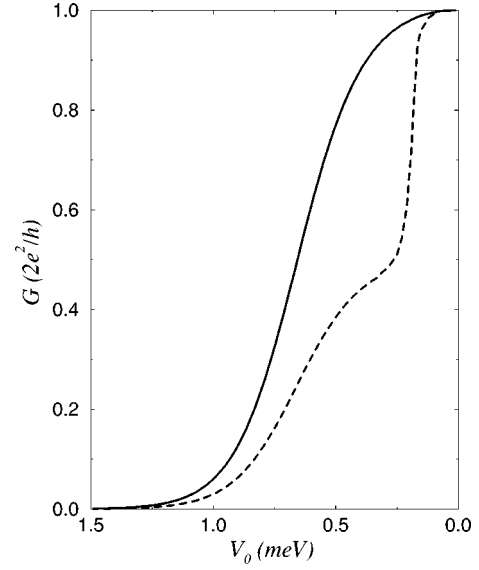


FIG. 4. The conductance G for a QPC versus the height V_0 of the saddle point. The Fermi level is $E_F=0.561$ meV relative to the lowest sublevel in the remote parts of the channel (“reservoirs”). The solid line corresponds to the noninteracting case and the dashed line to the interacting case.

$\leq 0.5(2e^2/h)$. For example, if the spontaneous spin polarization sets in at $G=0.7(2e^2/h)$ as observed in experiments, a second structure is to be expected for $G=0.2(2e^2/h)$. If an in-plane magnetic field B is applied, it follows from our model that the two structures will eventually merge on increasing B because of the Zeeman splitting. The additional spin polarization induced by this mechanism will become dominant at high fields implying a global polarization.

In conclusion, we have shown that spin polarization induced by exchange interactions is likely to occur in a QPC as the electron density is lowered towards pinch off by, for example, an applied gate voltage. Our model is based on the Kohn-Sham mean field approach. There is, therefore, the usual question of to what extent one can trust the new symmetry-broken solution, i.e., whether it is spurious or not. It is, of course, hard to prove one way or the other. Here we must, therefore, be guided by experience. Our problem is, in fact, similar to that of an impurity atom and the formation of local moments in a metallic host (electron gas jellium). In this case the spin-relaxed Kohn-Sham mean field approach yields local moments in good agreement with experiments (see, for example, Refs. 23–25). With such an approach it is also seen how the local moments disappear as the strength of the impurity relative the Fermi energy of the surrounding jellium is diminished. Qualitatively we thus obtain the same mechanism and, therefore, have faith in the true nature of our solutions. In the present case the onset of spin polarization manifests itself as an anomaly in the conductance. Evidently our calculations give qualitative support to the interpretation of measured anomalies. There appears, however, to be an important quantitative difference since our model predicts critical values for G that are sensitive to geometry. The critical value observed in Refs. 1 and 6 is $0.7(2e^2/h)$ or close to this value. One may think of a number of reasons for this discrepancy. Our theoretical results are based on quite a simplified model. Reservoirs, for example, are represented by

extended channels with one occupied mode only, the direction perpendicular to the interface is neglected, and so on. As already indicated, also the mean field approach may be too primitive to deal in a more detailed way with interaction effects when only very few electrons remain in the region of the QPC. At the same time, it is not yet firmly established from experiments that the conductance anomaly is independent of geometry. The lower value reported in Ref. 5 may be related to this point, but further experimentation with high-mobility devices is needed to settle the question about geometry. In summary, we suggest that spontaneous spin polarization in a QPC in the limit of low electron densities is a valid scenario that should be explored further in the ways just indicated. It should also be rewarding to go beyond the semi-classical form in Eq. (11) in order to include the oscillatory behavior in the effective, self-consistent potential as well as to allow for other delicate mean field effects.

Note added in proof. Recent self-consistent density-functional calculations predict that 3D nanowires of simple (nonmagnetic) metals undergo a transition to a spin-polarized state at critical radii [N. Zabala, M. J. Puska, and R. M. Nieminen (unpublished)]. Also the recent work on spontaneous spin polarization in circular quantum dots supports in a general way the mechanism proposed in this article [M. Koskinen, M. Manninen, and S. M. Reimann, Phys. Rev. Lett. **79**, 1389 (1997)].

ACKNOWLEDGMENTS

We are indebted to M. Pepper, K.J. Thomas, and J.T. Nicholls of the University of Cambridge, U.K., P. Ramvall and P. Omling of Lund University, Sweden, and R. Nieminen of Helsinki University of Technology, Finland, for informative discussions. This research was supported in part by the Swedish Natural Science Research Council.

-
- ¹K.J. Thomas, J.T. Nicholls, M.Y. Simmons, M. Pepper, D.R. Mace, and D.A. Ritchie, Phys. Rev. Lett. **77**, 135 (1996).
²B.J. van Wees, L.P. Kouwenhoven, E.M.M. Willems, C.J.P.M. Harmans, J.E. Mooij, H. van Houten, C.W.J. Beenakker, J.G. Williamson, and C.T. Foxon, Phys. Rev. B **43**, 12 431 (1991).
³J.E.F. Frost, M.Y. Simmons, M. Pepper, A.C. Churhill, D.A. Ritchie, and G.A. Jones, J. Phys.: Condens. Matter **5**, L599 (1993).
⁴P.L. McEuen, B.W. Alpenaar, and R.G. Wheeler, Surf. Sci. **229**, 312 (1990).
⁵R.D. Tscheuschner and A.D. Wieck, Superlattices Microstruct. **20**, 616 (1996).
⁶P. Ramvall, N. Carlsson, I. Maximov, P. Omling, L. Samuelsson, W. Seifert, Q. Wang, and S. Lourduoss, Appl. Phys. Lett. **71**, 918 (1997).
⁷N.K. Patel, J.T. Nicholls, L. Martín-Moreno, M. Pepper, J.E.F. Frost, D.A. Ritchie, G.A.C. Jones, Phys. Rev. B **44**, 13 549 (1991).
⁸C.L. Kane and M.P.A. Fisher, Phys. Rev. B **46**, 15 233 (1992).
⁹D.L. Maslov and M. Stone, Phys. Rev. B **52**, R5539 (1995).
¹⁰I. Safi and H.J. Schulz, Phys. Rev. B **52**, 17 040 (1995).
¹¹V.V. Ponomarenko, Phys. Rev. B **52**, 8666 (1995).
¹²S. Tarucha, T. Honda, and T. Saku, Solid State Commun. **94**, 413 (1995).
¹³C.-K. Wang and K.-F. Berggren, Phys. Rev. B **54**, R14 257 (1996).
¹⁴C. Herring, in *Magnetism*, edited by G.T. Rado and H. Suhl (Academic Press, New York, 1966), Vol. 4.
¹⁵S. Olszewski, Z. Phys. B **45**, 297 (1982).
¹⁶A. Gold and L. Calmels, Philos. Mag. Lett. **74**, 137 (1996).
¹⁷L. Calmels and A. Gold, Phys. Rev. B **56**, 1762 (1997).
¹⁸M. Büttiker, Phys. Rev. B **41**, 7906 (1990).
¹⁹L. Martín-Moreno, J.T. Nicholls, N.K. Patel, and M. Pepper, J. Phys.: Condens. Matter **4**, 1323 (1992).
²⁰See, for example, R. G. Parr and W. Yang, *Density-Functional Theory of Atoms and Molecules* (Oxford University Press, New York, 1989).
²¹F. Stern, Phys. Rev. Lett. **30**, 278 (1973).
²²L.I. Glazman and M. Jonson, J. Phys.: Condens. Matter **1**, 5547 (1989).
²³R.M. Nieminen and M. Puska, J. Phys. F **10**, L123 (1980).
²⁴N. Stefanou and N. Papanikolaou, J. Phys.: Condens. Matter **3**, 3777 (1991).
²⁵N. Papanikolaou, N. Stefanou, R. Zeller, and P.H. Dederichs, Phys. Rev. Lett. **71**, 629 (1993).